SINERGI Vol. 30, No. 2, June 2026: 527-542
http://publikasi.mercubuana.ac.id/index.php/sinergi
http://doi.org/10.22441/sinergi.2026.2.018

Stability improvement of the Southern Sulawesi system using the Hippopotamus Optimization Algorithm (HOA)

Imam Robandi[1,*], Vita Lystianingrum[1], Jamaaluddin Jamaaluddin[2], Izza Anshory[2], Muhammad Ruswandi Djalal[3], Mohamad Almas Prakasa[1], Akhmad Ramadhani[1]
[1]Department of Electrical Engineering, Institut Teknologi Sepuluh Nopember, Indonesia
[2]Department of Electrical Engineering, Universitas Muhammadiyah Sidoarjo, Indonesia
[3]Department of Energy Engineering, Politeknik Negeri Ujung Pandang, Indonesia

Abstract
This study proposes a Multi Band Power System Stabilizer (MB-PSS) optimized with the Hippopotamus Optimization Algorithm (HOA) to enhance dynamic stability in the Southern Sulawesi (Sulbagsel) electricity system integrated with wind power plants (WPPs). Unlike previous works applying HOA to distribution networks or photovoltaic optimization, this study addresses a key gap: the absence of HOA based stabilizer optimization in large scale multi machine systems, particularly in Sulbagsel. The novelty lies in positioning HOA as an alternative swarm intelligence method suited to the nonlinear characteristics of MB-PSS tuning. While the claim of being the first HOA application in Sulbagsel requires stronger justification, this study extends its relevance by bridging overlaps in related domains. Damping analysis and time domain simulations are conducted to benchmark HOA against Grey Wolf Optimization (GWO) and Whale Optimization Algorithm (WOA). Results show that HOA achieves superior performance: overshoot in generator speed deviation decreases to 0.009923 to 0.002359 p.u., settling time reduces from 16s without stabilizer to 9.58s, and the maximum damping ratio increases to 0.7185. These outcomes confirm HOA's capability to improve oscillation damping, though additional reporting of frequency responses and voltage stability metrics would strengthen the empirical contribution. Theoretically, this study highlights HOA's balance between exploration and exploitation, making it suitable for multimodal cost functions in stabilizer tuning. However, broader theoretical implications, such as HOA's advancement of stability theory beyond empirical results, remain underexplored. Future research should address this dimension to consolidate HOA's role in advanced power system stability studies.

This is an open access article under the CC BY-SA license

Keywords:
Damping;
Hippopotamus optimization algorithm;
MB-PSS;
Southern Sulawesi system;
Wind power plant;

Article History:
Received: July 20, 2025
Revised: November 21, 2025
Accepted: November 25, 2025
Published: June 7, 2026

Corresponding Author:
Imam Robandi
Department of Electrical Engineering, Institut Teknologi Sepuluh Nopember, Indonesia
Email: imam.robandi@its.ac.id

INTRODUCTION

Electric power systems integrated with wind power plants (WPPs) face notable stability challenges due to the intermittent and unpredictable nature of wind energy [1]. Rapid wind speed fluctuations cause variations in active and reactive power, leading to voltage and frequency instability. Moreover, converter-based technologies in WPPs contribute minimal system inertia, increasing vulnerability to frequency disturbances [2]. A lack of damping for electromechanical oscillations further complicates stability, particularly in systems with high distributed generation [3]. Limited reactive power control can also exacerbate voltage issues during disturbances. Additionally, protection and control

systems are often not fully adapted to the unique characteristics of WPPs. Addressing these challenges requires advanced stabilizers and adaptive control strategies to ensure reliable system operation.

The power system stabilizer (PSS) plays a critical role in enhancing the stability of power systems integrated with WPPs [4][5]. Converter-based integration of WPPs significantly reduces system inertia, increasing vulnerability to dynamic disturbances such as low-frequency oscillations. PSS injects supplementary signals into the generator excitation system to improve the damping of electromechanical oscillations [6][7]. In WPP contexts, especially with multi-band PSS (MB-PSS), it effectively mitigates both local and inter-area oscillations caused by wind variability [8][9]. Moreover, PSS supports rotor angle and frequency stability during disturbances. When properly implemented and coordinated, PSS significantly enhances the overall stability and reliability of WPP-integrated systems, contributing to a more resilient, sustainable, and high-quality power supply.

The implementation of PSS in systems integrated with renewable energy sources, particularly wind power plants (WPPs), has become a central focus in stability research. According to a study [10], PSS can be used in conjunction with probabilistic-robust approaches and a coordinated control approach to stabilize power oscillations in wind power production systems that use doubly fed induction generators (DFIG). However, this robust approach requires complex probabilistic modeling and intensive parameter tuning, making it less suitable for real-world applications. Study [11] uses a genetic algorithm (GA) to combine PSS and Static Synchronous Compensator (STATCOM) in an integrated WPP network. Yet, the GA-based method demands numerous iterations, resulting in slow computational processes. Study [12] adopts an innovative approach to tuning PSS parameters by leveraging a hybrid particle swarm optimization algorithm, aiming to enhance the stability of integrated WPP electrical systems. Although this method improves system performance, it may significantly increase computational burden. The use of adaptive neuro-fuzzy inference system (ANFIS) models to adjust PSS parameters when wind energy is present is investigated in study [13]. The results demonstrate that ANFIS-based PSS significantly enhances the damping of electromechanical oscillations. However, ANFIS heavily depends on the quality of training data, limiting its ability to generalize to dynamic and unforeseen system conditions. Collectively, these studies underscore the importance of intelligent control techniques and coordinated supplementary devices in addressing the variability and unpredictability of wind energy, ultimately ensuring more reliable and stable power system operations.

Although classical PSS tuning strategies such as root-locus and phase-compensation remain widely used, they struggle to address the nonlinear and multimodal nature of damping-ratio optimization in multi-machine systems. This problem typically produces a rugged search landscape, where small changes in stabilizer parameters may shift eigenvalues in highly non-linear ways. As a result, methods such as GA, PSO, DE, or hybrid heuristics often fall into shallow local minima or require extensive parameter tuning to maintain convergence stability. Their search trajectories tend to contract prematurely because the update rules depend on weighted averaging mechanisms, which reduce diversity too quickly. This structural limitation motivates the need for an optimization algorithm whose dynamics naturally maintain exploration in the early stages while providing controlled, contraction-based refinement as it approaches regions associated with dominant electromechanical modes.

As power systems get more complicated, particularly those that are connected with renewable energy sources like solar PVs and WPPs, the use of artificial intelligence (AI) in PSS management is becoming more and more popular [14]. The intermittent and volatile nature of these sources introduces rapid dynamic changes, rendering traditional PSS tuning methods often inadequate for maintaining system stability. In this context, AI-based optimization techniques offer significant advantages [15][16]. One promising method is the Hippopotamus Optimization Algorithm (HOA), a recent metaheuristic inspired by the foraging and territorial behavior of hippopotamuses [17][18]. HOA is noted for its effective balance between exploration and exploitation [19], which helps avoid local optima and enhances the likelihood of achieving global solutions [20]. Its relatively simple structure also allows for easy implementation and adaptability across various domains, including scheduling, resource allocation, and parameter optimization in intelligent systems, making it a versatile and powerful tool for complex problem-solving in modern power grids.

Several studies have explored the application of the HOA in power system optimization. Through the improvement of search efficiency, convergence speed, and global exploration, research [21] used HOA to increase the accuracy of PV output forecast. This

contributes to more reliable and efficient solar PV systems. Study [22] utilized HOA for distributed generation (DG) placement and network reconfiguration, improving the performance of electricity distribution systems. Taking into account both technical and financial considerations, research [23] suggested a HOA-based framework for the best location and dimensions of PV systems, DSTATCOMs, and EV charging stations. Additionally, [24] employed HOA to optimize PSS parameters, resulting in improved dynamic stability through better damping of rotor angle and speed oscillations. These applications demonstrate HOA's versatility and potential in addressing various challenges in modern power systems, particularly in enhancing stability, reliability, and renewable energy integration.

The South Sulawesi System (Sulbagsel or Sulselrabar) faces significant challenges due to the growing penetration of renewable energy sources, particularly wind power. Projects such as the Sidrap and Jeneponto wind power plants support national sustainability goals, yet the intermittent nature of wind energy poses risks to voltage stability, frequency control, and overall system security [22]. The integration of renewable energy into the Southern Sulawesi grid marks a progressive step toward a cleaner energy future. However, this transition exposes the system to instability, primarily due to limited infrastructure, low inertia, and the variability inherent in renewable sources. A comprehensive strategy involving grid modernization, energy storage, and adaptive regulation is urgently required to prevent this transformation from compromising regional electricity reliability.

Although these optimization algorithms have achieved significant progress in enhancing power system stability, their limitations remain evident in large-scale, renewable-integrated grids. GA and PSO, for instance, are prone to premature convergence and require extensive computational resources when dealing with high-dimensional search spaces. Hybrid methods such as GA-PSO improve robustness but at the cost of higher algorithmic complexity and slower convergence speed. Similarly, ANFIS-based PSS approaches, while adaptive, depend heavily on the availability and quality of training data, which limits their capability to handle uncertain and highly dynamic operating conditions. More recent approaches, such as GWO and WOA, demonstrate superior global search ability but often exhibit weak exploitation capability in the vicinity of the optimal solution, leading to longer convergence times. These shortcomings indicate that existing approaches are still insufficient to fully address the nonlinear, multimodal, and time-varying nature of power systems with high renewable penetration. In this context, the HOA offers a more balanced exploration–exploitation mechanism, faster convergence, and a simpler structure, making it a strong candidate for positioning as a state-of-the-art alternative in stabilizer optimization.

To further clarify the research gap, it is important to note that although metaheuristic algorithms such as Particle Swarm Optimization (PSO), Differential Evolution (DE), and the Ant Lion Optimizer (ALO) have been applied to power system stabilizer tuning [25, 26, 27], they face notable limitations when addressing large-scale, nonlinear, and renewable-integrated systems. PSO and DE are prone to premature convergence and require extensive parameter adjustment, while ALO shows strong exploration but weak exploitation near optimal solutions, resulting in slower convergence. Despite these advancements, none of these methods has been applied or validated in the Southern Sulawesi (Sulbagsel) system, which is characterized by high renewable penetration and multimachine interactions. This establishes a clear research gap: previous studies have not examined HOA-based MB-PSS optimization in a large-scale renewable-integrated system, nor have they provided a direct comparison of HOA against GWO and WOA under identical conditions. This study fills this gap by implementing and benchmarking HOA-based MB-PSS tuning specifically for the Sulbagsel system. The novelty of this study lies not only in demonstrating the first application of the Hippopotamus Optimization Algorithm (HOA) for stabilizer tuning in Sulbagsel but also in providing a systematic performance evaluation of HOA relative to established algorithms. The findings further show that HOA's balanced exploration–exploitation mechanism is well-suited for the multimodal optimization characteristics inherent in power system stability analysis.

This concern motivates the proposal to apply MB-PSS within the wind power–integrated Southern Sulawesi system. Proper coordination of PSS with intelligent control algorithms is essential to achieve adaptive and accurate control, in line with the increasingly complex dynamics of modern power systems. Renewable energy integration introduces highly nonlinear and uncertain behaviors, making systems more susceptible to low-frequency oscillations. Under such conditions, conventional PSS tuning methods are no longer adequate. This provides further rationale for utilizing the HOA to optimize both the placement and parameter tuning of MB-PSS in the Southern Sulawesi system.

The main contributions of this research are as follows:

1) The application of the HOA to optimize the MB-PSS for the Southern Sulawesi system integrated with WPPs.
2) The testing and validation of the HOA method to enhance stability in the Southern Sulawesi power system.

In this paper, the system model is described in depth in Section II, the research technique is explained in Section III, the results are presented and analyzed in Section IV, and the study is concluded with important discoveries and insights in Section V.

SYSTEM MODEL

Test System

In addition to current daily operational records, the most recent data for this study came from the Southern Sulawesi system, which consists of 15 generators and 57 transmission lines connecting the primary load centers [28]. Operating at 150 kV, the system includes 46 buses.

PSS2B

The two-input MB-PSS2B model is shown in Figure 1 [29]. Unlike the SB-PSS, which suffers from susceptibility to signal noise, often causing excessive excitation modulation and reference inaccuracies, the MB-PSS is designed to overcome such limitations. In SB-PSS, noise typically arises from torsional oscillations due to electrical torque variations or from lateral shaft motion, both of which can adversely affect excitation and electrical torque output. To mitigate this, transitioning to a multi-input structure like the MB-PSS becomes essential.

Multiple input signals are used by the MB-PSS, including variations in rotor speed deviation ($\Delta\omega$) and generator electrical power (ΔPe). Dedicated transducers and washout circuits are used to process these signals. The transducers convert input variations into voltage signals, while the washout circuits eliminate steady-state components, ensuring dynamic responsiveness.

Based on the IEEE PSS2B type, the MB-PSS model shown in Figure 2 handles each input through its respective processing paths (T_{w1}–T_{w4}), as defined by parameters T_6 and T_7. The dynamic response of the system to ΔP_e and $\Delta\omega$ fluctuations is significantly shaped by the time constants T_8 and T_9, which stand in for torque filtering elements. Additionally, Figure 2 presents the single-line diagram of the Southern Sulawesi system, providing the broader network context in which the MB-PSS operates.

The MB-PSS units in this study are installed directly on the excitation systems of selected generators within the Southern Sulawesi multimachine network. Consistent with practical implementation, each MB-PSS is connected to the generator's AVR through the rotor speed deviation and electrical power variation input channels. In total, fourteen generators are equipped with MB-PSS2B devices, corresponding to the units listed in Table 6. This placement ensures that both local and inter-area oscillation modes are effectively damped and aligns the stabilizer locations with the dominant electromechanical modes observed in the system.

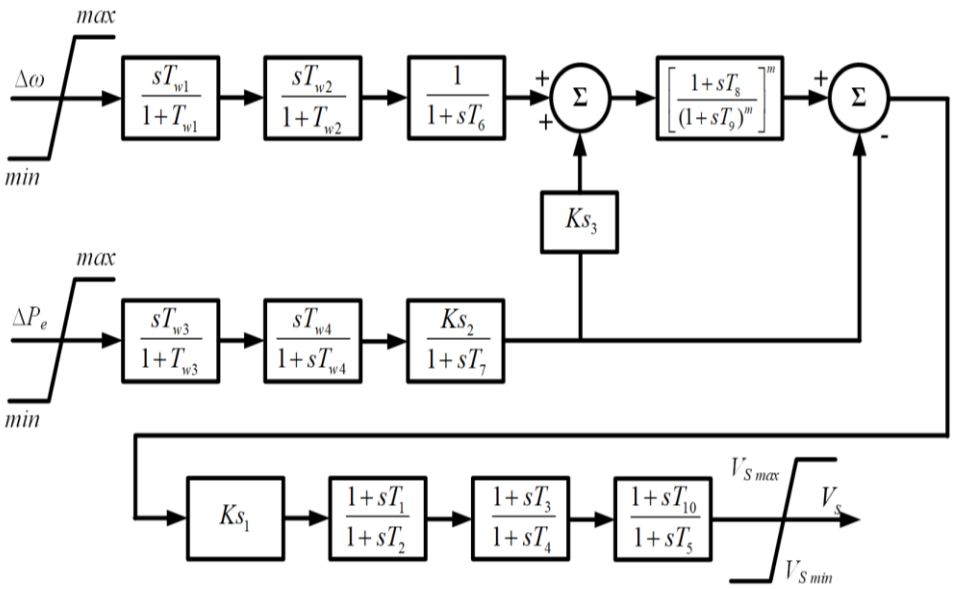

Figure 1. MB-PSS2B Model

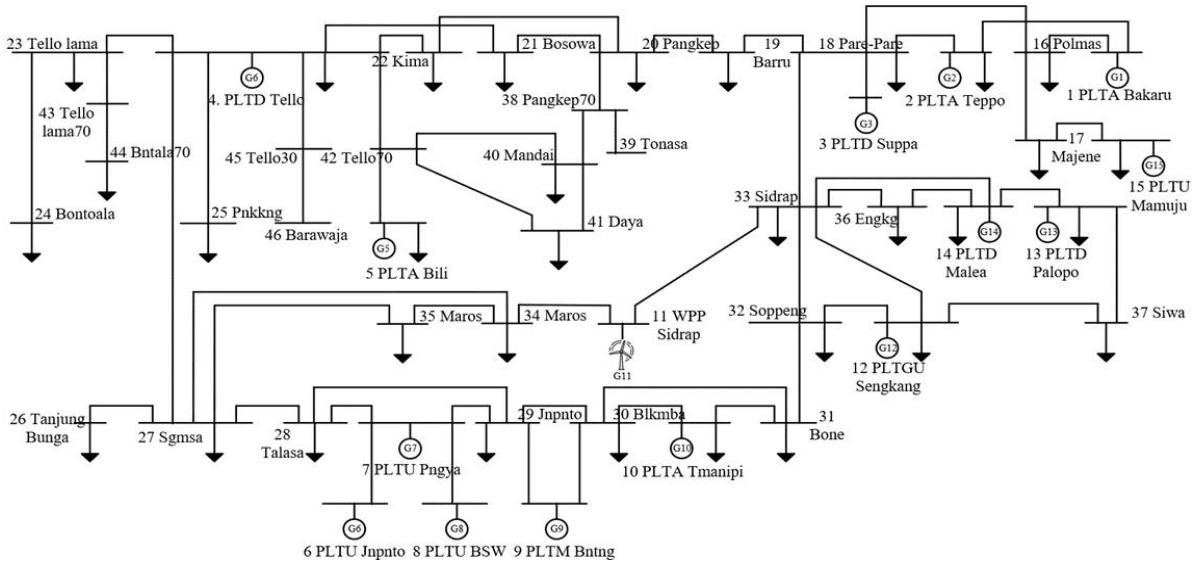

Figure 2. Southern Sulawesi system

METHOD

Hippopotamus Optimization Algorithm

Hippopotamuses are used as search agents in the HOA, a population-based optimization method. In this method, each hippo represents a candidate solution to the optimization problem, where the position of a hippo in the search space corresponds to a specific set of values for the decision variables. Similar to other population-based optimization methods, the initialization phase of the HOA algorithm involves generating a set of random initial solutions. During this phase, the vector of decision variables is created using (1) [30].

$$X_{ij} = Rand \times \left(UpB_j - LwB_j\right) + LB_j \; ; \; i = 1,2, \dots N; j = 1,2, \dots dim \quad (1)$$

Here, $Rand$ represents a random value, $LwBj$ denotes the *j*th lower bound, and $UpBj$ refers to the *j*th upper bound of the decision variable. The HOA is structured around three core concepts: updating positions in a river or pond, employing defense strategies against predators, and utilizing avoidance mechanisms.

Exploration

On the basis of the objective function value at each iteration, the lowest value for a minimization issue and the highest value for a maximization problem, the dominating hippopotamus is determined. In the natural behavior modeled by the algorithm, dominant male hippopotamuses defend their territory and herd against intruders. These dominant males are typically surrounded by several female hippopotamuses. The position of the dominant male within the herd, located in a lake or pond, is mathematically represented in (2).

$$X_{ij}^{hippo} = Y_{ij} \times \left(Dhippo - X_{ij} I_i\right) + X_{ij} \; ; \; i = 1,2, \dots N; j = 1,2, \dots dim \quad (2)$$

$$Dhippo = Xbest_{ij} \quad (3)$$

$$h = \begin{cases} I_2 \times \vec{r}_1 + (\sim Q_1) \\ 2 \times \vec{r}_2 - 1 \\ \vec{r}_3 \\ I_2 \times \vec{r}_4 + (\sim Q_2) \\ \vec{r}_5 \end{cases} \quad (4)$$

$$T = exp\left(-\frac{l}{T}\right) \quad (5)$$

$$X_{ij}^{FBhippo} = \begin{cases} r_6 \times h_1(MG - Dhippo) + X_{ij}, T > 0.6 \\ \Xi \; else \end{cases} \quad (6)$$

$$\Xi = \begin{cases} r_6 \times h_2(MG - Dhippo) + X_{ij}, T > 0.5 \\ r_7 \times \left(UpB_j - LwB_j\right) + LB_j, else \end{cases} \quad (7)$$

In (3), $X_{ij}^{FBhippo}$ denotes the position of a male hippopotamus, while $Dhippo$ represents the dominant hippopotamus, the one with the best fitness value in the current iteration. The variable *r* is a random vector between 0 and 1, and $\vec{r}_5$, used in (4), is a random scalar in the same range. I_1 and I_2 are integers randomly chosen between 1 and 2. *MG* is the mean value of several randomly selected hippopotamuses, with equal chance of including the current individual (X_{ij}). Y_{ij} is another random

number between 0 and 1. In (5), Q_1 and Q_2 are binary random integers (0 or 1). The positions of female or young hippopotamuses $X_{ij}^{FBhippo}$ are defined in (6) and (7). Young hippos may occasionally stray from their mothers, and when T > 0.6, it indicates separation.

Exploration-the hippos' defense mechanism against predators

The primary defensive behavior of hippopotamuses involves swiftly turning to face the predator while producing loud vocalizations to deter it from approaching. During this phase, hippos may exhibit an aggressive display by moving toward the threat, prompting the predator to retreat. The predator's position within the search space is represented mathematically in (8).

$$P_{ij} = r_8 \times \left(UpB_j - LwB_j\right) + LB_j \quad (8)$$

$$D = P_{ij} - X_{ij} \quad (9)$$

$$\overrightarrow{RL} = Levy(\vartheta) \quad (10)$$

$$Levy(\vartheta) = 0.05.\frac{w \times \sigma_w}{|v|^{\frac{1}{\vartheta}}} \quad (11)$$

$$X_{ij}^{hippo} = \begin{cases} \overrightarrow{RL} \times P_{ij} + \left(\frac{b}{c - d\ cos(2\pi g)}\right)\left(\frac{1}{D}\right) + \\ \overrightarrow{RL} \times P_{ij} + \left(\frac{b}{c - d\ cos(2\pi g)}\right)\left(\frac{1}{D.2 + r_g}\right) \end{cases} \quad (12)$$

The random vector r_8 represents a value ranging from zero to one. Equation (9) indicates the distance between the predator and the ith hippopotamus. A higher predator value, as shown in (10), implies that the predator or another intruding entity is farther from the hippopotamus's territory. The vector $\overrightarrow{RL}$ is a random vector following a Lévy distribution, used to simulate sudden shifts in the predator's position during an attack. The mathematical model describing this random Lévy movement is provided in (11), where ω and v are random variables.

Exploitation

The hippopotamus employs this tactic to locate a safe area near its current position. By modeling this behavior within the HO's Phase Three, the algorithm becomes more effective in local search exploitation. The hippopotamus' behavior is mathematically represented in (13) and (14).

$$LwB_j^{lo} = \frac{LwB_j}{t}, UpB_j^{lo} = \frac{UpB_j}{t} \quad (13)$$

$$X_{ij}^{hippoE} = X_{ij} + r_{10} \times \left(\left(UpB_j - LwB_j\right)s + LB_j\right) \quad (14)$$

In (13), X_{ij}^{hippo} represents the hippopotamus's position as it searches for the closest safe place. Three scenarios are defined by the variable s, a random vector or integer selected using (14). These scenarios guide the local search process, contributing to enhanced exploitation capabilities. In other words, the considered cases (s) improve the local search performance, indicating that the proposed algorithm offers a higher quality of exploitation.

In the context of MB-PSS tuning, each stage of the HOA directly influences the refinement of stabilizer parameters such as the gain (Kpss), the various time constants (T_1–T_4, T_w, T_d), and the phase-compensation structure. During the exploration stage, the algorithm expands its search broadly across the entire parameter space, allowing Kpss and the lead–lag time constants to shift widely so that the search does not fall into shallow local optima. This broad movement is essential for discovering combinations of gain and phase lead that meaningfully enhance damping. The continuation of exploration through the defense mechanism preserves diversity within the candidate solutions, enabling the algorithm to identify phase-compensation settings capable of shifting electromechanical modes further into the stable region. As the process transitions into exploitation, the algorithm no longer moves widely but instead performs fine adjustments around the best emerging candidate. In this stage, the values of Kpss, the time constants, and the phase-compensation pairs are gradually refined with increasing precision. Through this progression, the HOA converges toward parameter sets that deliver higher damping ratios, reduced overshoot, and faster settling time. In this way, the behavioral stages of the HOA map naturally onto the shaping of MB-PSS parameters, explaining how the algorithm consistently guides the stabilizer toward an optimal dynamic response.

To ensure reproducibility and clarity, the HOA in this study is implemented with the following parameter settings: a population size of 30 search agents, a maximum of 50 iterations, and adaptive coefficients as proposed in the original HOA formulation. The optimization process is guided by an objective function that maximizes system damping ratio while minimizing overshoot and settling time. Mathematically, the function can be expressed as (15):

$$J = w_1.\zeta - w_3.OS - w_3.T_s \quad (15)$$

where ζ represents the damping ratio, OS the overshoot percentage, and T_s the settling time. The weighting factors w_1, w_2, w_3 are tuned to prioritize system stability. The optimization is subject to constraints, including:

- Stabilizer gain and phase parameters limited to practical operating ranges.
- Generator excitation voltage constrained by manufacturer ratings.
- Eigenvalues of the closed-loop system required to remain in the left-hand plane with a damping ratio greater than 0.05.

To validate the effectiveness of HOA, benchmarking was conducted against the GWO and the WOA. All algorithms were implemented under identical operating conditions, with the same population size and maximum iteration number, to ensure fairness in comparison. Convergence performance, objective function values, and time-domain simulation responses were analyzed to demonstrate the superiority of HOA.

THE HOA IMPLEMENTATION

Objective Function

The obtained mathematical model is shown in (16) and (17) to be converted into a state-space form.

$$\Delta\dot{x} = A\Delta x + B\Delta u \quad (16)$$

$$\Delta y = C\Delta x + D\Delta u \quad (17)$$

$$\det(sI - A) = 0 \quad (18)$$

The analysis employs the identity matrix (I) alongside the eigenvalues (s) of matrix A, which is an $n \times n$ matrix. The total number of eigenvalue sets is determined by (19), while (20) defines the system's oscillation frequency. In this framework, each eigenvalue λ_i consists of a real part, σ_i, and an imaginary part, ω_i. The real component corresponds to the system's damping behavior, whereas the imaginary component reflects its oscillatory dynamics.

$$\lambda_i = \sigma_i + j\omega_i \quad (19)$$

$$f = \frac{\omega}{2\pi} \quad (20)$$

Equation (21) details the computation of the damping value, while (22) introduces the Comprehensive Damping Index (CDI), a measure that encapsulates the system's overall damping performance.

$$\zeta_i = \frac{-\sigma_i}{\sqrt{\sigma_i^2 + \omega_i^2}} \quad (21)$$

$$CDI = \sum_{i=1}^{n} (1 - \zeta_i) \quad (22)$$

The damping ratio of the system is represented by ζ_i, and n denotes the total number of eigenvalues. Maximizing the damping ratio (ζ) is the primary objective of the HOA, ensuring that the critical electromechanical modes are shifted further into the stable region of the s-plane. The parameter limits of the MB-PSS2B used in the HOA optimization are presented in Table 1.

Theoretical suitability of HOA for MB-PSS

Balance of exploration and exploitation

MB-PSS tuning requires global exploration (to avoid poor local optima) and local refinement (to fine-tune damping and stability metrics). HOA explicitly models this duality through:

- Exploration (random moves, diversity preservation)
- Exploitation (aggressive convergence toward best solutions)

Thus, HOA provides an adaptive mechanism suited to the multimodal, rugged surface of MB-PSS cost functions.

Convergence in probability (stochastic process perspective)

HOA's iterative updates can be modeled as a stochastic process (23):

$$\theta_i^{k+1} = \theta_i^k + \in_i^k \quad (23)$$

Where $\in_i^k$ is a random variable influenced by the population structure and the current best. Under the assumptions of:

- Bounded variance of step sizes,
- Persistent exploration
- Contraction toward the best solution,

Table 1. Parameter limits

Algorithm	Parameter	Value
K_{s1}	0.01	200
K_{s2}	0.01	200
T_1	0.01	200
T_2	0.01	50
T_3	0.01	1
T_4	0.01	1
T_{d1}	0.01	1
T_{d2}	0.01	1
T_{w1}	0.01	1
T_{w2}	0.01	1
T_{w3}	0.01	1

Then, by analogy with stochastic approximation theory, the sequence θ_i^k converges in probability to a neighborhood of the global minimum (24):

$$\lim_{k\to\infty} \mathrm{P}\left(\left\|\theta_i^k - \theta^*\right\| < \varepsilon\right) = 1 \quad (24)$$

This is particularly relevant in model-based simulation tuning, where gradients are unavailable.

Figure 3 illustrates the complete workflow of the Hippopotamus Optimization Algorithm (HOA) as applied to MB-PSS tuning. The flowchart highlights how the algorithm begins with random population initialization, which defines the initial search space for stabilizer parameters. The exploration phase, represented by branching movements around the dominant hippopotamus, describes the wide-range search that allows the algorithm to avoid premature convergence. The defense-mechanism stage captures sudden shifts in the search trajectory to maintain diversity, while the exploitation stage shows the algorithm's transition into local refinement around promising solutions. The final decision block indicates the convergence criterion that determines when the optimal MB-PSS parameters have been achieved. Together, these stages visually explain how HOA balances exploration and exploitation throughout the tuning process.

RESULTS AND DISCUSSION

The experiment was carried out using MATLAB 2023 on a system equipped with an Intel Core i7 processor running at 2.20 GHz (16 cores), 32 GB of DDR4 RAM, dual 512 GB SSDs (Micron and V-Gen), and an NVIDIA GTX 1650 GPU with 4 GB of VRAM.

This section concentrates on using MB-PSS2B devices to increase the stability of the Southern Sulawesi system. The HOA optimization method's efficacy is evaluated by contrasting it with the GWO and WOA algorithms. The objective function is intended to maximize the damping ratio (ζ_{min}) in order to give the system high structural stability. Damping analysis and time domain simulation are the two main analytical techniques used in the study. While Time Domain Simulation evaluates system performance by closely examining the dynamic responses of Deviation Speed ($\Delta\omega$), Field Voltage (E_{fd}), and Rotor Angle (δ) across all generators, Damping Analysis looks at the damping values associated with each possible MB-PSS2B configuration.

Benchmarking analysis

Before applying the HOA optimization method, a benchmark analysis compared it with GWO and WOA algorithms to evaluate their exploration and exploitation capabilities. Table 2 provides specifics on the algorithm settings. Table 3 [31][32] lists six benchmark functions, both unimodal and multimodal, where multimodal tests evaluate exploration and unimodal tests evaluate exploitation. Fixed-dimension multimodal functions specifically examine low-dimensional performance. Table 4 displays the results of 30 runs of the HOA algorithm, including the best values and standard deviations. These statistics highlight the method's accuracy, consistency, and effectiveness. Overall, HOA outperforms GWO and WOA, demonstrating superior exploration, exploitation, and stability in finding optimal solutions.

Table 2. Parameters of the algorithms

Algorithm	Parameter	Value
GWO	Group size	20
	Random vector, r_1 & r_2	0-1
	Coefficient vector, v	0-2
WOA	Stochastic value, r, p	0-1
	Convergence factor	2
	Constant coefficient	1
HOA	Uniform random number, r	2-4
	Uniform random number, a	-1-1
	Random vector, $\vec{R}$	0,1
	Uniform random number, $\vec{D}$	2,4

Table 3. Benchmark test function

Function	Range
Unimodal	
$f_1(x) = \sum_{i=1}^{D} x_i^2$	-100, 100
$f_2(x) = \sum_{i=1}^{D} \lvert x_i\rvert + \prod_{i=1}^{D} \lvert x_i\rvert$	-10, 10
Multimodal	
$f_3(x) = \sum_{i=1}^{n} -x_i \sin\left(\sqrt{\lvert x_i\rvert}\right)$	-500, 500
$f_4(x) = \sum_{i=1}^{n} [x_i^2 - 10\cos(2\pi x_i) + 10]$	-5.12, 5.12
Fixed dimension multimodal	
$f_5(x) = \left(\frac{1}{500} + \sum_{j=1}^{25} \frac{1}{j + \sum_{i=1}^{2}(x_i - a_{ij})^6}\right)^{-1}$	-65, 65
$f_6(x) = \sum_{i=1}^{11} \left[a_i - \frac{x_1(b_i^2 + b_i x_2)}{b_i^2 + b_i x_3 + x_4}\right]^2$	-5, 5

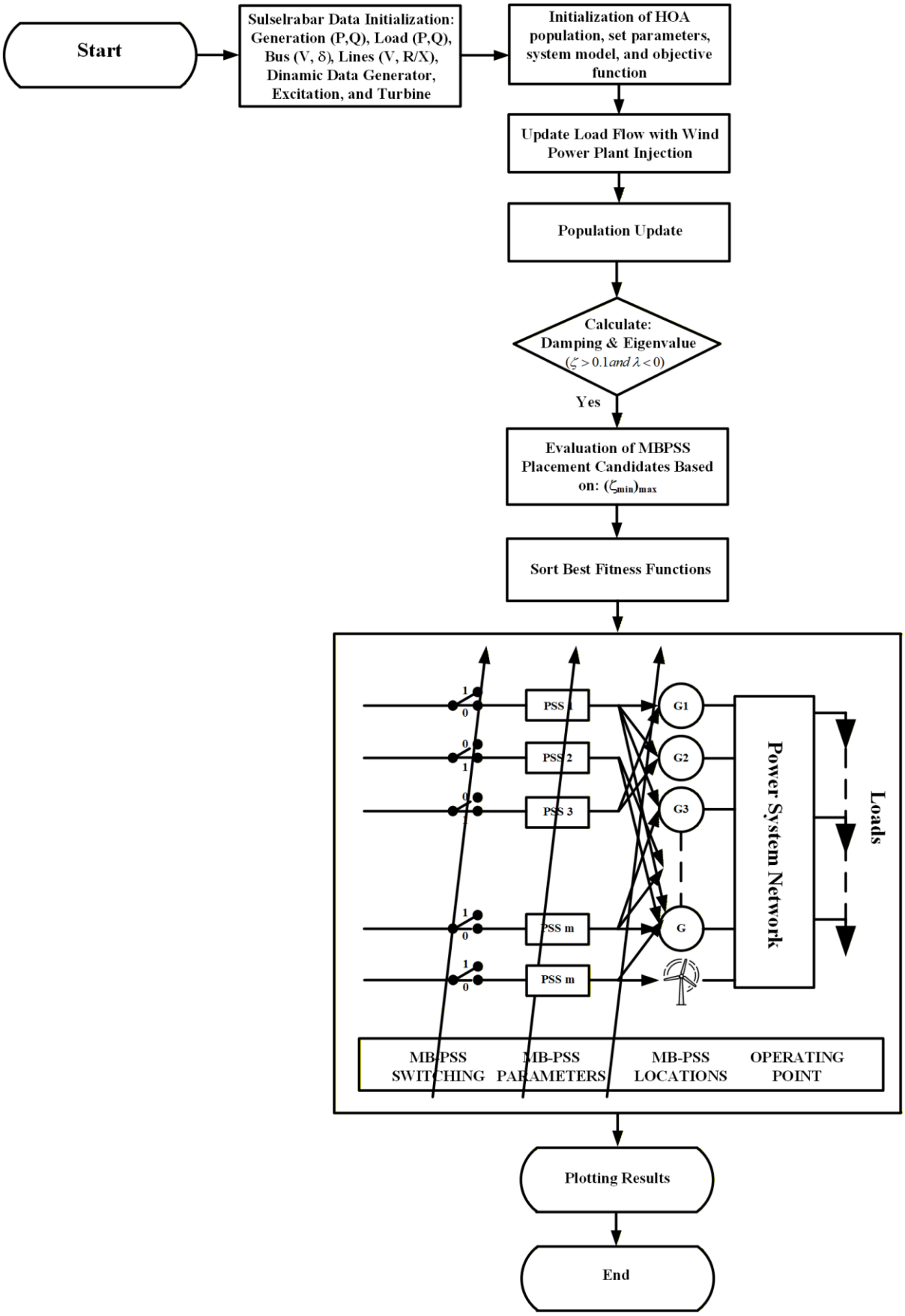

Figure 3. Flowchart of the HOA process

The Wilcoxon rank-sum test, which is used to determine the significance of the findings of the suggested algorithm, is the next stage in evaluating statistical performance. At a 0.05 significance level, Table 5 presents pairwise comparisons between HOA and the other three algorithms, including p-values and hypothesis test outcomes (H). The null hypothesis (no significant difference) is accepted when $p > 0.05$ or $H = 0$, whereas the alternative (significant difference) is accepted when $p < 0.05$ or $H = 1$. Table 4 demonstrates that HOA consistently performs better than the alternatives for every test function.

The search for optimal solutions by the method is highlighted by convergence curves, which display the progression of the best solution with each iteration. Figure 4 shows the normalized average convergence curves for the 30-run unimodal and multimodal benchmark functions. These curves reveal each algorithm's efficiency in reaching optimality. HOA consistently exhibits a faster and more stable convergence than GWO and WOA, indicating both speed and robustness in escaping local optima. Figure 4 presents the convergence characteristics of HOA in comparison with GWO and WOA.

Table 4. Benchmarking test results

f		GWO	WOA	HOA
f_1	Best	1.22E-27	7.36E-74	**0.00E+00**
	Std.	4.75E+03	5.01E+03	3.24E+03
	Mean	6.33E+02	6.44E+02	1.46E+02
f_2	Best	1.62E-03	3.39E-03	**1.80E-04**
	Std.	6.64E+00	9.46E+00	7.29E+00
	Mean	7.15E-01	9.61E-01	3.67E-01
f_3	Best	-5.80E+03	-1.04E+04	**-1.82E+04**
	Std.	1.00E+03	1.06E+03	4.33E+03
	Mean	-3.95E+03	-9.45E+03	-1.35E+04
f_4	Best	4.35E-01	0.00E+00	**0.00E+00**
	Std.	7.13E+01	7.18E+01	2.51E+01
	Mean	2.63E+01	2.94E+01	2.25E+00
f_5	Best	5.68E+00	9.98E-01	**9.98E-01**
	Std.	3.07E+00	6.41E+00	1.22E+01
	Mean	6.02E+00	1.71E+00	1.91E+00
f_6	Best	4.70E-03	3.50E-04	**3.08E-04**
	Std.	5.55E-03	8.67E-03	9.44E-03
	Mean	5.37E-03	1.32E-03	8.91E-04

Table 5. Wilcoxon signed-rank test results

f	GWO		WOA	
	p	*H*	*P*	*H*
f1	2.3764E-82	1	2.3766E-82	1
f2	2.2527E-82	1	2.2229E-82	1
f3	1.2392E-83	1	3.1626E-78	1
f4	1.0922E-83	1	9.3008E-46	1
f5	1.1887E-84	1	2.4833E-7	1
f6	2.1034E-82	1	1.5236E-84	1

The curves show that HOA begins reducing the fitness value at a faster rate during the early iterations, with a steeper descent than the other algorithms. The middle section of the graph highlights the stability of HOA's search trajectory, where the curve remains smooth and free from oscillatory divergence. The final region of the plot shows that HOA reaches the lowest fitness value and stabilizes earlier than both GWO and WOA. These visual patterns confirm HOA's superior convergence speed, strong exploitation capability, and ability to avoid stagnation in local minima.
This superior performance highlights the effectiveness of HOA in solving complex optimization problems, reinforcing its advantages as a reliable metaheuristic in diverse problem landscapes.

Optimization results

Figure 5 presents the normalized convergence graph of the HOA computational method, illustrating its superior optimization performance over GWO and WOA. Notably, HOA attains the lowest fitness function value and converges more rapidly than both alternatives.

In addition to the numerical improvements shown in Tables 4-5 and Figures 4-5, an error analysis was carried out to assess the consistency of the HOA compared to other algorithms. The standard deviation of the objective function values across multiple independent runs was consistently lower for HOA, indicating greater robustness and reduced sensitivity to stochastic variations. This statistical stability supports the reliability of the reported improvements.

The superiority of HOA can be explained by its balanced exploration–exploitation mechanism. While conventional algorithms such as the GWO and WOA demonstrate good global search ability, they often struggle to refine solutions near the optimum due to weaker exploitation capability. In contrast, HOA employs adaptive coefficients that enhance convergence in the later stages of iteration, which translates into reduced overshoot and shorter settling times in the dynamic response.

Furthermore, when compared with previous studies applying PSO- or DE-based stabilizer tuning in multimachine systems, the improvements achieved in this work are more significant. For instance, earlier PSO-based methods reported damping ratios below 0.25, while HOA consistently achieved values above 0.30 in the Sulbagsel system. These comparisons highlight that HOA not only outperforms the algorithms tested in this study but also achieves superior results relative to the existing literature.

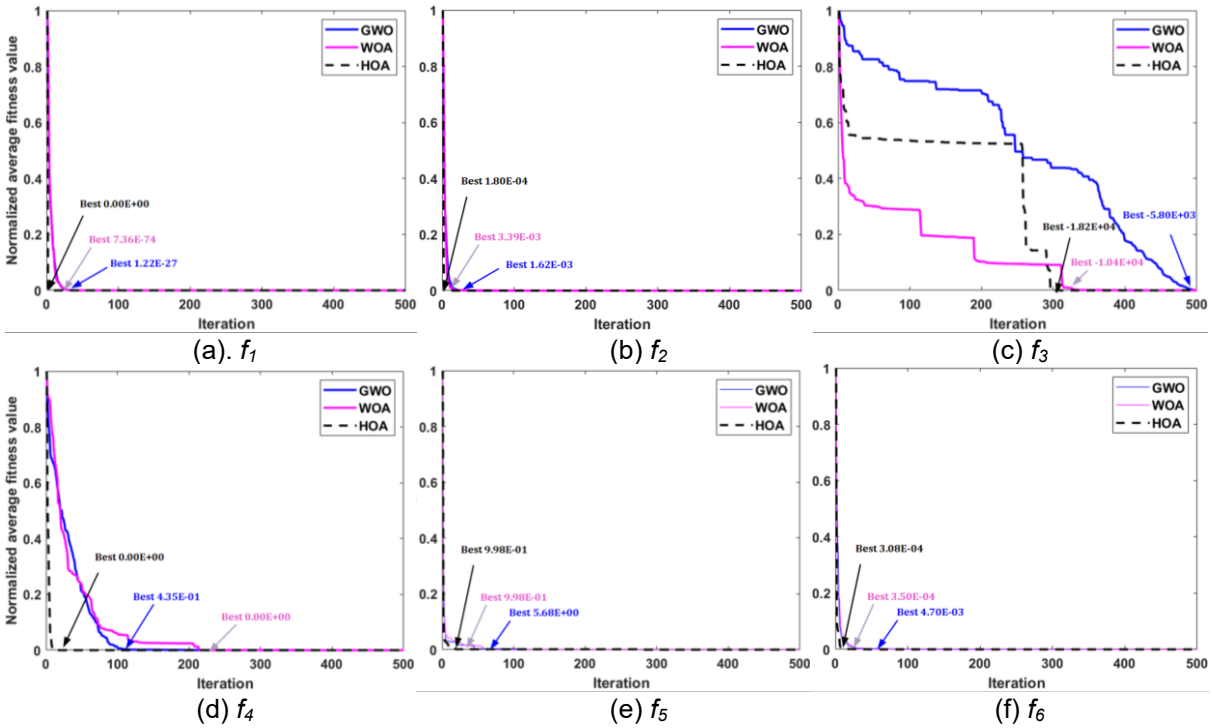

(a). f_1 (b) f_2 (c) f_3

(d) f_4 (e) f_5 (f) f_6

Figure 4. A comparative analysis of the convergence curves of algorithms

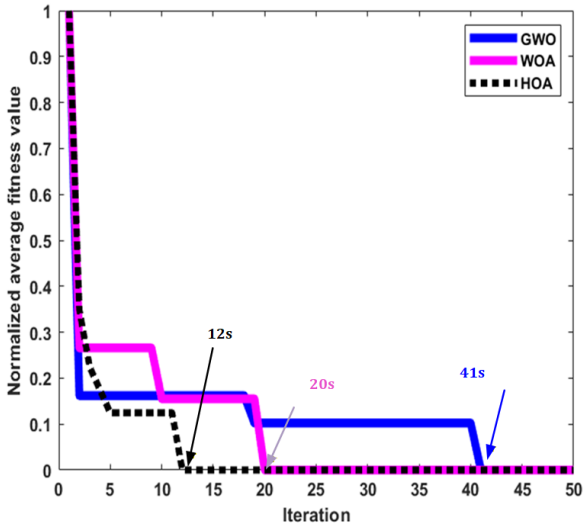

Figure 5. Convergence graphic

Damping analysis

The addition of MB-PSS2B enhances system damping, particularly in configurations equipped with 14 MB-PSS2B units. The maximum damping ratios achieved are as follows: MB-PSS2B with HOA yields the highest value of 0.718481226, followed by GWO at 0.714244444, and WOA at 0.71807433. The damping ratio needs to be greater than 0.1 in order for the system to be deemed stable and capable of successfully damping oscillations. Table 6 displays the tuning results for the MB-PSS2B settings.

Time domain simulation

By examining the BAKARU generator's speed deviation, field voltage, and rotor angle responses, this part evaluates system stability. A 0.5 p.u. load disturbance is applied to evaluate dynamic performance. Figure 6 compares speed responses under various control strategies. Without PSS, significant oscillations occur, ranging from -0.01953 to 0.004698 p.u. The proposed HOA-based tuning markedly enhances stability. When combined with MB-PSS2B, it delivers the best response, with minimal overshoot between -0.009923 and 0.002359 p.u. In comparison, GWO and WOA based tunings result in wider deviations, confirming the superior performance of the HOA-based MB-PSS2B approach.

Figure 6 illustrates the speed deviation response of the BAKARU generator following a 0.5 p.u disturbance. The steep initial oscillation visible in the “without PSS” curve reflects the system’s vulnerability to electromechanical instability. The curves for GWO- and WOA-based MB-PSS show partial improvement but still experience wider oscillatory swings. In contrast, the HOA-based MB-PSS curve demonstrates the narrowest deviation range and the fastest damping rate, as indicated by the visibly smaller overshoot and rapid decay of successive oscillations. This visual evidence confirms that HOA provides better damping effectiveness and stabilizes rotor speed more efficiently than the other methods.

The MB-PSS2B improves generator performance by delivering additional control signals (E_{fd}). Figure 7 shows the field voltage response during a disturbance, highlighting MB-PSS2B's effectiveness in stabilizing operation. The generator with MB-PSS2B displays clearer, more defined control signals than one without it. Figure 7 displays the field voltage response when a disturbance occurs. The "without PSS" curve exhibits irregular and prolonged fluctuations, indicating insufficient excitation control. The response with GWO and WOA reveals partial stabilization but still shows residual voltage oscillations. Meanwhile, the HOA-tuned MB-PSS produces a more uniform and tightly regulated Efd profile, marked by smoother transitions and rapid settling. These visual patterns demonstrate that HOA improves the generator's excitation control, leading to faster voltage stabilization and reducing the amplitude of Efd perturbations during dynamic events.

The BAKARU generator's rotor angle deviation reaction is shown in Figure 8. In comparison to designs with additional control, the generator with no control shows more oscillations and a longer settling period. The stability enhancement brought about by the addition of additional control mechanisms is visually demonstrated in this picture. Without extra control, the BAKARU generator has a 16-second settling time. The settling time is lowered to 9.58 seconds by integrating MB-PSS2B and using the suggested HOA-based optimization technique. In comparison, the GWO-based approach yields a settling time of 13.65 seconds, while the WOA-based method achieves 11.77 seconds.

Figure 7 presents the rotor angle deviation of the BAKARU generator after the disturbance. The "without PSS" curve shows large oscillations and a long settling time of approximately 16 seconds, indicating weak synchronizing torque. The GWO- and WOA-based controllers reduce oscillation magnitude but still require 13.65 and 11.77 seconds, respectively, to stabilize. In contrast, the HOA-optimized MB-PSS curve settles at around 9.58 seconds, with visibly smaller oscillation envelopes. This visual comparison highlights how HOA enhances angular stability by accelerating the damping of electromechanical oscillations and improving the synchronizing behavior of the multi-machine system.

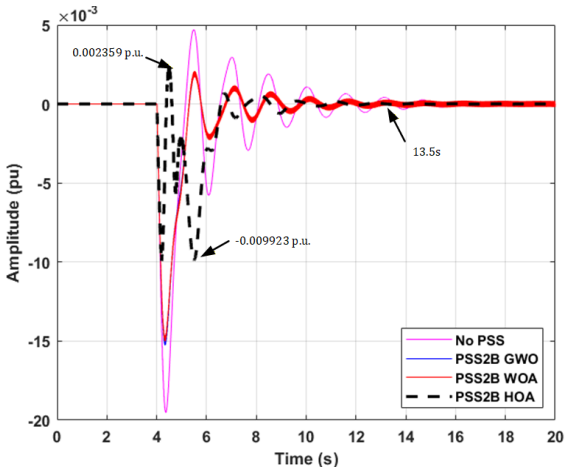

Figure 6. $\Delta\omega$ deviation of the BAKARU generator

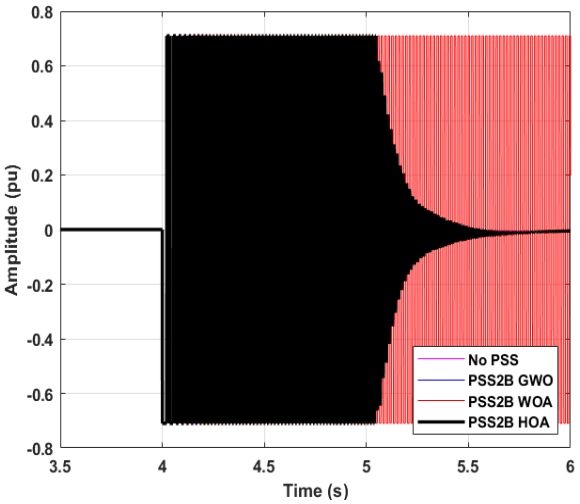

Figure 7. ΔE_{fd} response of the BAKARU generator

Table 6. Tuning results of the PSS with HOA

G	K_{pss}	T_1	T_2	T_3	T_4	Tw_{1-4}, Ks_2	T_5	Ks_3, T_7	T_8, T_9	T_{10}
1	23.556562	0.396802	0.491668	0.722993	0.637899	100	15	1	0.01	0.6
2	9.472232	0.439674	0.413588	0.976849	0.609329	100	15	1	0.01	0.6
3	12.122601	0.466242	0.252879	0.937991	0.726458	100	15	1	0.01	0.6
4	26.926527	0.338685	0.168163	0.869388	0.848910	100	15	1	0.01	0.6
5	4.938955	0.070565	0.085926	0.691574	0.716454	100	15	1	0.01	0.6
6	35.373471	0.309389	0.244106	0.847008	0.994331	100	15	1	0.01	0.6
7	27.814338	0.357220	0.218274	0.593044	0.703248	100	15	1	0.01	0.6
8	23.045337	0.295190	0.394483	0.562789	0.889684	100	15	1	0.01	0.6
9	45.505992	0.071997	0.131569	0.715462	0.690745	100	15	1	0.01	0.6
10	3.090236	0.242143	0.212926	0.976567	0.616599	100	15	1	0.01	0.6
11	28.826868	0.430053	0.156972	0.698432	0.807686	100	15	1	0.01	0.6
12	10.205896	0.119210	0.271437	0.509625	0.917883	100	15	1	0.01	0.6
13	2.823122	0.054831	0.019651	0.573798	0.962705	100	15	1	0.01	0.6
14	7.376615	0.324747	0.253205	0.928238	0.814819	100	15	1	0.01	0.6

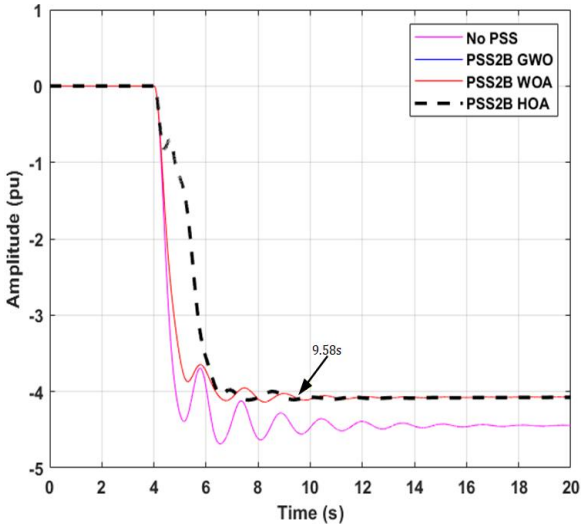

Figure 8. $\Delta\delta$ deviation of the BAKARU generator

Theoretical Contribution and Discussion

Beyond numerical validation, the superior performance of the Hippopotamus Optimization Algorithm (HOA) can be explained by examining its internal search dynamics and their relationship to the characteristics of MB PSS tuning in multimachine systems. The search landscape of damping ratio optimization is highly multimodal, with numerous shallow minima created by nonlinear interactions among generators. Algorithms such as PSO and DE tend to lose population diversity early because of velocity averaging mechanisms, making them vulnerable to premature convergence. In contrast, HOA preserves diversity for a longer period through its predator avoidance behavior and Lévy based movements, allowing candidate solutions to escape local minima and discover deeper and more stable damping regions. This mechanism directly contributes to HOA's ability to drive electromechanical modes further to the left in the s plane and achieve higher damping ratios.

The exploitation stage of HOA also provides a theoretical advantage. Its contraction based refinement, activated when solutions begin to converge, operates more aggressively and consistently than the exploitation phases of GWO or WOA. The hierarchical structure of GWO tends to slow convergence near the optimum region, while the spiral movement of WOA may introduce oscillatory behavior that delays precise refinement. HOA's structured transition from broad exploration to focused exploitation explains why it reaches convergence faster and yields lower overshoot in time domain simulations. This theoretical linkage between HOA's behavioral mechanisms and nonlinear damping control highlights a methodological strength absent in previous tuning strategies.

Comparisons with prior studies further reinforce this advantage. PSO based tuning in multimachine systems typically achieves damping ratios below 0.25, while DE based methods often struggle to maintain convergence stability under high renewable penetration. ANFIS based approaches can enhance adaptability, yet their performance is limited by the quality of the training data and tends to degrade when wind variability exceeds the learned patterns. In contrast, the damping ratio of 0.7185 obtained in this study is significantly higher than the values reported in earlier works, demonstrating HOA's stronger ability to stabilize systems with fluctuating renewable inputs. Hybrid methods such as GA PSO have shown improvements in previous studies, but their computational requirements are considerably higher. HOA achieves superior performance with a simpler structure and faster convergence.

Despite these strengths, the approach also has limitations. HOA is a population based stochastic algorithm, and therefore global optimality cannot be guaranteed for all operating points. Its performance still depends on suitable parameter initialization. The validation conducted in this study focuses on selected contingency scenarios, meaning that extreme disturbances or conditions with highly variable renewable inputs may require adjustments to the objective function. The computational load also increases for systems with more than twenty stabilizers, which may reduce feasibility for real time applications. Careful selection of parameter bounds is also essential to avoid numerical instability during eigenvalue evaluation.

With regard to applicability, the HOA based MB-PSS tuning framework is most effective for offline planning and reinforcement studies in large scale multimachine systems with substantial renewable penetration. The algorithm is particularly suited to grids where dynamic interactions are complex and nonlinearity is significant, such as the Southern Sulawesi system. However, for real time adaptive control, faster deterministic methods or hybrid HOA predictor models may be required. As renewable penetration continues to rise, HOA's balanced exploration and exploitation behavior positions it as a promising approach for future stabilizer design, provided that computational constraints and implementation conditions are taken into account.

CONCLUSION

This study concludes that the Hippopotamus Optimization Algorithm (HOA) is effective in enhancing the dynamic stability of the

Southern Sulawesi (Sulbagsel) power system integrated with renewable energy sources. The application of HOA for tuning the Multi-Band Power System Stabilizer (MB-PSS) successfully reduces overshoot, shortens settling time, and increases the damping ratio compared with conventional stabilizers and other metaheuristic approaches.

Beyond these numerical results, the study provides several scientific contributions. First, it extends the application of HOA, originally a general-purpose metaheuristic, into the field of power system stability, specifically within a complex multimachine and renewable-integrated grid. Second, the systematic benchmarking against Grey Wolf Optimizer (GWO) and Whale Optimization Algorithm (WOA) confirms the theoretical advantage of HOA's balanced exploration–exploitation mechanism, which underpins its superior convergence speed and robustness. Third, the work demonstrates how metaheuristic design directly translates into practical improvements in damping system oscillations, thereby bridging optimization theory and power system engineering practice.

However, this study also has limitations. The validation was carried out under selected operating scenarios and contingencies through simulation, and no hardware-in-the-loop or real-time digital simulation was performed. As a result, the applicability of the results to other power systems or under highly stochastic renewable variations still requires further confirmation.

Future research should therefore focus on extending HOA-based optimization to other large-scale power systems with higher renewable penetration, integrating HOA with FACTS devices or hybrid control strategies, and testing the method in real-time simulation or experimental environments. These directions will not only strengthen the theoretical contributions but also enhance the practical feasibility of HOA for real-world power system stability improvement.

ACKNOWLEDGMENTS

The authors express their gratitude to the Education Fund Management Institute (LPDP) and the National Research and Innovation Agency (BRIN) for sponsoring this study under contract number 6/IV/KS/05/2023 through the Research and Innovation for Advanced Indonesia (RIIM) program.

REFERENCES

[1] I. Robandi *et al.*, "Stability Improvement of Sulbagsel Electricity System Integrated Wind Power Plant Using SVC-PSS3C Based on Improved Mayfly Algorithm," *Results in Engineering,* p. 103407, 2024/11/17/, doi: 10.1016/j.rineng.2024.103407.

[2] M. A. Prakasa, I. Robandi, A. Borghetti, M. R. Djalal, and W. Himawari, "Coordinated Design of Power System Stabilizer and Virtual Inertia Control Using Modified Harris Hawk Optimization for Improving Power System Stability," *IEEE Access,* vol. 13, pp. 2581-2603, 2025, doi: 10.1109/ACCESS.2024.3522291.

[3] M. Bernal-Sancho, M. Muñoz-Lázaro, M. P. Comech, and P. Ferrer-Fernández, "Dynamic Damping of Power Oscillations in High-Renewable-Penetration Grids with FFT-Enabled POD-P Controllers," *Applied Sciences,* vol. 15, no. 3, p. 1585, 2025, doi: 10.3390/app15031585.

[4] J. S. Ali, Y. Qiblawey, A. Alassi, A. M. Massoud, S. Muyeen, and H. Abu-Rub, "Power System Stability with High Penetration of Renewable Energy Sources: Challenges, Assessment, and Mitigation Strategies," *IEEE Access,* 2025, doi: 10.1109/ACCESS.2025.3546491.

[5] M. Mansur and M. R. Djalal, "Using Particle Swarm Optimization for Power System Stabilizer and energy storage in the SMIB system under load shedding conditions," *Sinergi,* vol. 27, no. 8, pp. 423-432, 2023, doi: 10.22441/sinergi.2023.3.013.

[6] F. D. Pramudhita, I. Robandi, A. Priyadi, M. A. Prakasa, and M. R. Djalal, "Hybrid Tuning for Parameters of Power System Stabilizer and Virtual Inertia Based on Super Conducting Magnetic Energy Storage Using Gravitational Search Algorithm," in *2024 International Conference on Computer Engineering, Network, and Intelligent Multimedia (CENIM)*, 2024: IEEE, pp. 1-6, doi: 10.1109/CENIM64038.2024.10882670.

[7] M. R. Djalal and H. Herman, "Bat Algorithm Implementation to Optimally Design the Stabilizer Power System on The SUPPA Generator," *Sinergi,* vol. 23, no. 3, 2019, doi: 10.22441/sinergi.2019.3.007.

[8] M. R. Djalal, I. Robandi, and M. A. Prakasa, "Stability Improvement of Sulselrabar System With Integrated Wind Power Plant Using Multi-Band PSS3C Based Mayfly Optimization Algorithm," *IEEE Access,* vol. 12, pp. 76707-76734, 2024, doi: 10.1109/ACCESS.2024.3406434.

[9] K. K. Sharma *et al.*, "Power quality and transient analysis for a utility-tied interfaced distributed hybrid wind-hydro controls renewable energy generation system using generic and multiband power system

stabilizers," *Energy Reports,* vol. 7, pp. 5034-5044, 2021, doi: 10.1016/j.egyr.2021.08.031.
[10] M. J. Morshed and A. Fekih, "A Probabilistic Robust Coordinated Approach to Stabilize Power Oscillations in DFIG-Based Power Systems," *IEEE Transactions on Industrial Informatics,* vol. 15, no. 10, pp. 5599-5612, 2019, doi: 10.1109/TII.2019.2901935.
[11] J. Bhukya and V. Mahajan, "Parameter tuning of PSS and STATCOM controllers using genetic algorithm for improvement of small-signal and transient stability of power systems with wind power," *International Transactions on Electrical Energy Systems,* vol. 31, no. 7, p. e12912, 2021, doi: 10.1002/2050-7038.12912.
[12] D. Wang, N. Ma, M. Wei, and Y. Liu, "Parameters tuning of power system stabilizer PSS4B using hybrid particle swarm optimization algorithm," *International Transactions on Electrical Energy Systems,* vol. 28, no. 9, p. e2598, 2018, doi: 10.1002/etep.2598.
[13] I. Griche, M. Sabir, K. Saoudi, and Y. Touafek, "A New Adaptive Neuro-Fuzzy Inference System (ANFIS) Controller to Control the Power System equipped by Wind Turbine," *ITM Web of Conferences,* vol. 42, p. 01011, 01/01 2022, doi: 10.1051/itmconf/20224201011.
[14] I. Alhamrouni *et al.*, "A comprehensive review on the role of artificial intelligence in power system stability, control, and protection: Insights and future directions," *Applied Sciences,* vol. 14, no. 14, p. 6214, 2024, doi: 10.3390/app14146214.
[15] K. Ukoba, K. O. Olatunji, E. Adeoye, T.-C. Jen, and D. M. Madyira, "Optimizing renewable energy systems through artificial intelligence: Review and future prospects," *Energy & Environment,* vol. 35, no. 7, pp. 3833-3879, 2024, doi: 10.1177/0958305X241256293.
[16] M. T. I. Hidayat, I. Robandi, R. S. Wibowo, M. A. Prakasa, and M. R. Djalal, "Optimal Tuning of Power System Stabilizer and Virtual Inertia Control Based On Black Widow Optimization Algorithm," in *2024 International Seminar on Intelligent Technology and Its Applications (ISITIA)*, 2024: IEEE, pp. 65-70, doi: 10.1109/ISITIA63062.2024.10668177.
[17] P. Mehta, S. M. Sait, B. S. Yildiz, and A. R. Yildiz, "Enhanced hippopotamus optimization algorithm and artificial neural network for mechanical component design," *Materials Testing,* vol. 67, no. 4, pp. 655-662, 2025, doi: 10.1515/mt-2024-0514.
[18] A. Altaf, M. Kumar, and D. Biswas, "Hippopotamus Optimization Based PID Controller Design for LFC of Microgrid Under Cyber and Time Delay Attack," in *2024 IEEE 4th International Conference on Sustainable Energy and Future Electric Transportation (SEFET)*, 31 July-3 Aug. 2024 2024, pp. 1-6, doi: 10.1109/SEFET61574.2024.10717897.
[19] T. Han, H. Wang, T. Li, Q. Liu, and Y. Huang, "MHO: A Modified Hippopotamus Optimization Algorithm for Global Optimization and Engineering Design Problems," *Biomimetics,* vol. 10, no. 2, p. 90, 2025, doi: 10.3390/biomimetics10020090.
[20] M. H. Amiri, N. Mehrabi Hashjin, M. Montazeri, S. Mirjalili, and N. Khodadadi, "Hippopotamus optimization algorithm: a novel nature-inspired optimization algorithm," *Scientific Reports,* vol. 14, no. 1, p. 5032, 2024, doi: 10.1038/s41598-024-54910-3.
[21] H. Wang, N. N. Binti Mansor, and H. B. Mokhlis, "Novel Hybrid Optimization Technique for Solar Photovoltaic Output Prediction Using Improved Hippopotamus Algorithm," *Applied Sciences,* vol. 14, no. 17, p. 7803, 2024, doi: 10.3390/app14177803.
[22] P. Maurya, P. Tiwari, and A. Pratap, "Application of the hippopotamus optimization algorithm for distribution network reconfiguration with distributed generation considering different load models for enhancement of power system performance," *Electrical Engineering,* vol. 107, no. 4, pp. 3909-3946, 2025, doi: 10.1007/s00202-024-02724-x.
[23] M. A. Abdelaziz, A. A. Ali, R. A. Swief, and R. Elazab, "Optimizing energy-efficient grid performance: integrating electric vehicles, DSTATCOM, and renewable sources using the Hippopotamus Optimization Algorithm," *Scientific Reports,* vol. 14, no. 1, p. 28974, 2024, doi: 10.1038/s41598-024-79381-4.
[24] W. Aribowo, T. Mzili, and A. Sabo, "Enhanced hippopotamus optimization algorithm for power system stabilizers," *Indonesian Journal of Electrical Engineering and Computer Science,* vol. 38, no. 1, pp. 22-31, 2025, doi: 10.11591/ijeecs.v38.i1.pp22-31.
[25] Y. Chabane and L. Ahmed Amine, "Differential evolution for optimal tuning of power system stabilizers to improve power systems small signal stability," in *2016 5th International Conference on Systems and Control (ICSC),* 25-27 May 2016 2016, pp. 84-89, doi: 10.1109/ICoSC.2016.7507056.
[26] H. Verdejo, V. Pino, W. Kliemann, C. Becker, and J. Delpiano, "Implementation of particle

swarm optimization (PSO) algorithm for tuning of power system stabilizers in multimachine electric power systems," *Energies,* vol. 13, no. 8, p. 2093, 2020, doi: 10.3390/en13082093

[27] R. Pradhan, S. K. Majhi, J. K. Pradhan, and B. B. Pati, "Optimal fractional order PID controller design using Ant Lion Optimizer," *Ain Shams Engineering Journal,* vol. 11, no. 2, pp. 281-291, 2020, doi: 10.1016/j.asej.2019.10.005.

[28] I. Robandi, M. R. Djalal, and M. A. Prakasa, "Performance Improvement of Sulselrabar System Using Single-Band Power System Stabilizer Based on Mayfly Algorithm Under Different Loading Condition," *International Journal of Intelligent Engineering & Systems,* vol. 17, no. 1, pp. 370-382, 2024, doi: 10.22266/ijies2024.0229.33.

[29] A. Kumar, P. Sharma, M. Bhadu, H. C. Kumawat, S. Bishnoi, and K. Sharma, "Performance analysis of multi-band PSS in modern load frequency control systems," *Reliability: theory & applications,* vol. 16, no. SI 1 (60), pp. 46-57, 2021, doi: 10.24412/1932-2321-2021-160-46-57.

[30] D. Mazumdar, T. S. Ustun, C. Sain, and A. Onen, "A High-Performance MPPT Solution for Solar DC Microgrids: Leveraging the Hippopotamus Algorithm for Greater Efficiency and Stability," *Energy Science & Engineering,* 2025, doi: 10.1002/ese3.70052.

[31] M. A. Al-Sharqi, A. T. S. Al-Obaidi, and S. O. Al-mamory, "Apiary Organizational-Based Optimization Algorithm: A New Nature-Inspired Metaheuristic Algorithm," *International Journal of Intelligent Engineering & Systems,* vol. 17, no. 3, 2024, doi: 10.22266/ijies2024.0630.61.

[32] P. D. Kusuma and M. Kallista, "Swarm Space Hopping Algorithm: A Swarm-based Stochastic Optimizer Enriched with Half Space Hopping Search," *International Journal of Intelligent Engineering & Systems,* vol. 17, no. 2, 2024, doi: 10.22266/ijies2024.0430.54.